Quasi Multi-Pulse Back-to-Back Static Synchronous Compensator Employing Line Frequency Switching 2-Level GTO Inverters

A.M. Vural, K.C. Bayindir

***Abstract*—**Back-to-back static synchronous compensator (BtB-STATCOM) consists of two back-to-back voltage-source converters (VSC) with a common DC link in a substation. This configuration extends the capabilities of conventional STATCOM that bi-directional active power transfer from one bus to another is possible. In this paper, VSCs are designed in quasi multi-pulse form in which GTOs are triggered only once per cycle in PSCAD/EMTDC. The design details of VSCs as well as gate switching circuits and controllers are fully represented. Regulation modes of BtB-STATCOM are verified and tested on a multi-machine power system through different simulation cases. The results presented in the form of typical time responses show that practical PI controllers are almost robust and stable in case of start-up, set-point change, and line faults.

***Keywords*—**Flexible AC Transmission Systems (FACTS); Back-to-Back Static Synchronous Compensator (BtB-STATCOM); quasi multi-pulse voltage source converter; active power transfer; voltage control

I. Introduction

VSC-HVDC systems are utilized for asynchronous network interconnections and back-to-back ac system linking [1]-[4]. However, BtB-STATCOM is a multi-converter FACTS device, considered as a VSC-HVDC system without long DC transmission [5]. With the feature of bi-directional real power transfer between adjacent buses, the conventional shunt reactive power compensation feature [6]-[7] is extended and the integration of large-scale renewable energy sources with the grid is also possible [8]. Two or more VSCs are coupled through their DC sides in a substation so that long HVDC lines or cables are not required for coupling [9]-[14]. Although, there is a great number of STATCOM installations, it can be noted a few BtB-STATCOM installations. SDG&E Talega STATCOM with BtB extension is a good application example, which is rated at ± 100 MVA, has also a 50 MW of real power transfer capacity from East Bus to West Bus [11]. Another application example supports ± 36 MVar reactive power injection with a real power transfer capacity of 35 MW [12]. High controllability and the ability to control real/reactive powers independently at each terminal make converter-based transmission attractive in many applications like the emerging interconnection with renewable energy sources. [15]- [17]. Also, it is able to reverse the power flow without any dynamic modifications of the control structure while taking benefits of the four-quadrant converter operation. In this study, BtB-STATCOM with two high power VSCs with a common DC link is proposed and designed in a powerful electromagnetic transient program, PSCAD. Each VSC consists of eight six-pulse converters and switching elements (GTO) are triggered at fundamental frequency of 60 Hz. This configuration brings two main advantages: 1) Voltage and current stresses on each GTO is fairly decreased using multi-converter structure, and 2) Each GTO is triggered at fundamental frequency of 60 Hz. High frequency pulse width modulation which brings two-degrees of freedom to the control parameters is avoided in this study due to the high switching losses in high power applications. Pulses have equal width, so the second control degree is attained by using a phase shift technique between converter groups of VSC. The design details of the power circuit, pulse generating circuits, and controllers are presented in great detail and BtB-STATCOM embedded with a multi-machine power system is tested and verified for step-change commands and for two types of faults. In summary, this work has the following attributes: Realistic high power VSC model is designed for FACTS applications in PSCAD/EMTDC environment including magnetic interface. The switching frequency is kept as low as possible being fundamental frequency to minimize converter losses. "phase command calculation method" proposed by Hagiwara et al. [18] is modified and adapted to independent real/reactive power control for each VSC. The studied model can also be extended to VSC based HVDC transmission studies by incorporating DC line/cable models. With back-to-back converters it is also possible to supply a fixed amount of bi-directional power flow in micro grid applications.

A.M. Vural is with the Department of Electrical and Electronics Engineering, Gazikent University, Gaziantep, Turkey (phone: +90-342-2118080; fax: +90-342-2118081; e-mail: metevural@hotmail.com).

K.C. Bayindir is with the Department of Electrical and Electronics Engineering, Cukurova University, Adana, Turkey (phone: +90-322-3386868; fax: +90-322-3386326; e-mail: kcbayindir@yahoo.com).

II. Principle of BTB-STATCOM Operation

Two VSCs, connected in parallel through shunt transformers (Tr_{1-2}) with the power grid, is tied by a DC link (represented by capacitor C) which enables real power transfer

in both directions. The circuit topology is shown as Fig. 1(a). Each VSC synthesizes three-phase controllable voltage signals ($V_{sh1\text{-}2}$) with controllable phase angles ($\theta_{sh1\text{-}2}$) by employing self-commutative high power switches (GTO). With this configuration, real/reactive currents are injected into the buses for real power transfer ($P_{transfer1\text{-}2}$) and reactive power support ($Q_{inj1\text{-}2}$). Based on Fig. 1(b), a set of steady-state operating constraints for BtB-STATCOM is defined in (1). $P_{inj1\text{-}2}$ is the resultant net power injection from each VSC into the network. $P_{loss1\text{-}2}$ is the sum of switching losses and coupling transformer losses of each VSC, respectively. DC capacitor voltage should be regulated to a constant value by keeping the sum of $P_{transfer1}$ and $P_{transfer2}$ at zero in steady-state. This constraint is also expressed in (1).

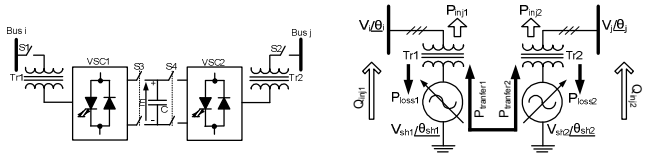

Fig. 1 General model of BtB-STATCOM connected to power grid and respective real/reactive power injections

$$\left.\begin{aligned} &P_{inj1} - P_{transfer1} - P_{loss1} - P_{loss2} = 0 \\ &P_{inj2} - P_{transfer2} = 0 \\ &P_{transfer1} + P_{transfer2} = 0 \end{aligned}\right\} \quad (1)$$

The injected current from VSC1 into Bus i, under the assumption that no resistive component between them can be derived as

$$\vec{I}_{sh1} = \frac{V_{sh1}\angle\theta_{sh1} - a_1^{-1}V_i\angle\theta_i}{jX_{sh1}} \quad (2)$$

where a_1 is the turns ratio of transformer, Tr1 and X_{sh1} represents equivalent reactance of Tr1 and coupling reactor. The real and reactive power injections of VSC1 into power system can be described using the following equations.

$$P_{inj1} + jQ_{inj1} = 3\vec{V}_i\vec{I}_{sh1}^{\,*} \quad (3)$$

Symbol (*) denotes complex conjugate. After some modifications, (3) is written in open form where P_{inj1} and Q_{inj1} are explicitly defined as functions of system parameters and VSC1 control parameters. Voltages are split into their *d*- and *q*- axis components ($V_D = V\cos\theta$, $V_Q = V\sin\theta$) in the rotating reference frame.

$$P_{inj1} = \frac{3a_1^{-1}}{X_{sh1}}\left(V_{iD}V_{sh1Q} - V_{iQ}V_{sh1D}\right) \quad (4)$$

$$Q_{inj1} = \frac{3a_1^{-1}}{X_{sh1}}\left[V_{iD}\left(V_{sh1D} - a_1^{-1}V_{iD}\right) + V_{iQ}\left(V_{sh1Q} - a_1^{-1}V_{iQ}\right)\right] \quad (5)$$

Since there is symmetry, the same sort of equations can be derived for VSC2. The injected current from VSC2 into Bus j is;

$$\vec{I}_{sh2} = \frac{V_{sh2}\angle\theta_{sh2} - a_2^{-1}V_j\angle\theta_j}{jX_{sh2}} \quad (6)$$

where a_2 is the turns ratio of transformer, Tr2 and X_{sh2} represents equivalent reactance of Tr2 and coupling reactor. The real and reactive power injections of VSC2 into power system are described in open form using the following equations.

$$P_{inj2} = \frac{3a_2^{-1}}{X_{sh2}}\left(V_{jD}V_{sh2Q} - V_{jQ}V_{sh2D}\right) \quad (7)$$

$$Q_{inj2} = \frac{3a_2^{-1}}{X_{sh2}}\left[V_{jD}\left(V_{sh2D} - a_2^{-1}V_{jD}\right) + V_{jQ}\left(V_{sh2Q} - a_2^{-1}V_{jQ}\right)\right] \quad (8)$$

The BtB-STATCOM DC link capacitor dynamics can be expressed as follows with harmonics neglected. E is the DC link voltage presented in Fig. 1(a).

$$\frac{dE}{dt} = \frac{1}{CE}\left(\sum_{m=1}^{3}P_{inj,m} - \sum_{m=1}^{3}P_{loss,m}\right) \quad (9)$$

III. BTB-STATCOM POWER CIRCUIT DESIGN

The power circuit schematic of each VSC (VSC1-2) of BtB-STATCOM is shown in Fig. 2. Each VSC is built up by combining four 12-pulse converter units (1,2,3,4) that are connected in parallel through their DC link with an energy storing DC capacitor (C=0.2 F) to achieve quasi multi-pulse operation. Each 12-pulse converter unit is comprised by two two-level six-pulse converters, each of which consists of six GTOs with reverse-parallel diodes.(GTO/diode ON/OFF resistances are 0.005Ω/1.0E8Ω). Based on required blocking voltage / peak current ratings, parallel and/or series combinations of GTOs are possible with auxiliary circuits. Multiple connections can also be employed for reasons of economy and easy availability of switches with lower ratings. In this study, only one GTO per arm is considered as the switching device to decrease simulation time. AC terminals of upper and lower six-pulse converters (a-b, c-d, e-f, g-h) are connected in Δ and Y, respectively. The firing pulses then need a relative phase shift of 30º between them. Three single-phase three-winding transformers are used as magnetic structure to couple AC outputs of two neighboring 12-pulse converter units (1-2) and (3-4). They work together as quasi 24-pulse (4x6) converter unit (converter M-N). AC output voltage waveforms of converter M and N are electro-magnetically added by two single-phase transformers for each phase to obtain a quasi multi-pulse waveform. This magnetic interface also couples VSC output voltage with the transmission level with no requirement to an extra shunt coupling transformer. Each upper side VSC of four twelve-pulse units is phase shifted by 7.5º. With this respect, the following displacement angles; 7.5º, 0.0º, -7.5º, and -15º are applied to the gating signals of each twelve-pulse unit. The design specifications of the magnetic interfaces are also represented in Fig. 2. Phase shifting transformers especially for true-multi pulse converters are not required in this work. Since one DC link with a single capacitor exists, the configuration is highly suitable for back-to-back VSC operations in FACTS applications [19]-[20]. This situation can

bring lower cost when practical aspects are considered. Moreover, it has total harmonic distortion (THD) similar to that of true multi-pulse one with equal number of switching devices [20]. Multi-pulse converter model is more accurate than existing low-order or average models.

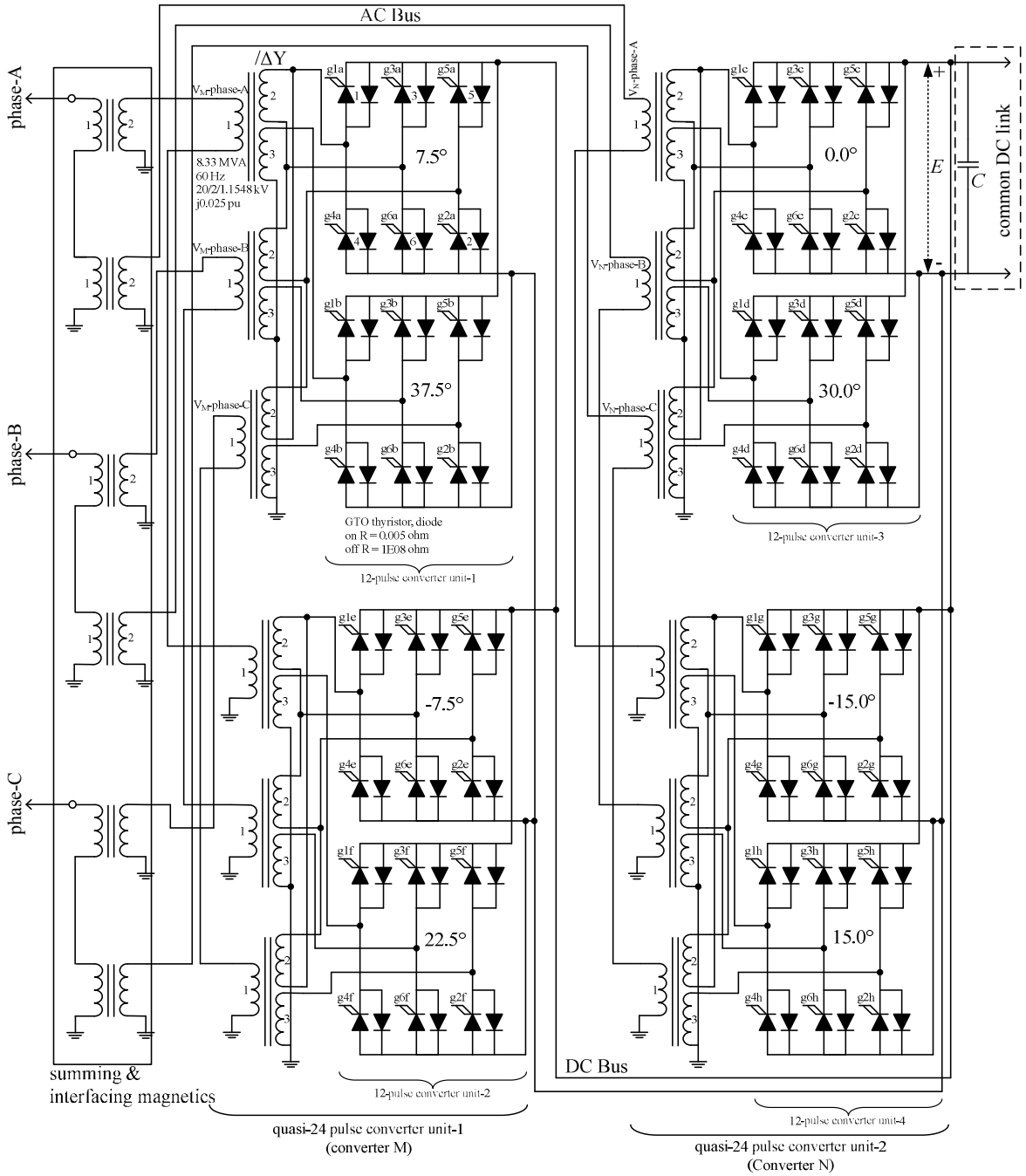

Fig. 2 Schematic of power circuit configuration of quasi multi-pulse VSC

IV. BTB-STATCOM CONTROL

Since pulse-width-modulation will not be used due to high switching losses, we have only fixed-width square wave with fundamental frequency @ 60 Hz to trigger GTOs. To attain an extra control degree, the only control parameter is phase shift that can be applied to these pulses. Pulse generation is based on this fact that the VSC configuration is decomposed into two main converter groups (converter M-N) as mentioned in Section 3. By referring to voltage phasors drawn in Fig. 3, the required magnitude and phase angle of the VSC output voltage (V_X) is obtained by suitable phase angle adjustments (α, δ) given in (10)-(11) and summing output voltage vectors of converter M-N (V_M ,V_N), given in (12) [18]. With this respect,

V_M is shifted with respect to *d*-axis by (α-δ), while V_N is shifted with respect to *d*-axis by (-α-δ). In BtB-STATCOM, two-degrees of freedom (voltage magnitude and phase angle) for each VSC are obtained with this manner which implies required real/reactive power injections from each VSC. V_D^{ref} and V_Q^{ref} expressed in (10)-(11) for each VSC are calculated from the PI control blocks, shown in Fig. 4. PI parameters for VSC1 are as follows: (DC voltage controller: K_{p1}=0.1, T_{i1}=0.01), (AC voltage controller: K_{p2}=0.8, T_{i2}=0.001). PI parameters for VSC2 are as follows: (Real power transfer controller: K_{p3}=0.8, T_{i3}=0.01), (AC voltage controller: K_{p4}=0.8, T_{i4}=0.001). The advantage of using such simple scheme is that it is a generic standard control method which is highly suitable for practical applications [21].

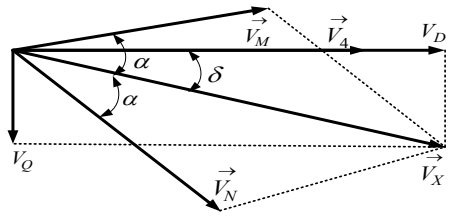

Fig. 3 Voltage vectors of Group M-N in rotating reference frame

$$\alpha = \tan^{-1}\sqrt{\frac{\left(V_M + V_N\right)^2 - \left(V_D^{ref}\right)^2 - \left(V_Q^{ref}\right)^2}{\left(V_D^{ref}\right)^2 + \left(V_Q^{ref}\right)^2}} \tag{10}$$

$$\delta = \tan^{-1}\frac{V_Q^{ref}}{V_D^{ref}} \tag{11}$$

$$\left.\begin{aligned}\vec{V}_M &= V_M\angle\phi_M = V_M\angle(\alpha-\delta)^\circ\\ \vec{V}_N &= V_N\angle\phi_N = V_N\angle-(\alpha+\delta)^\circ\end{aligned}\right\} \tag{12}$$

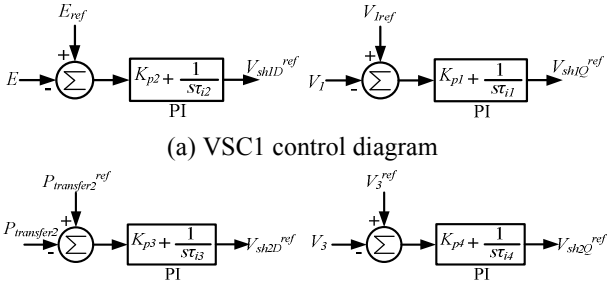

(a) VSC1 control diagram

(b) VSC2 control diagram

Fig. 4 PI control schemes of BtB-STATCOM

Pulse generating circuit for each six-pulse converter units (a-h) is presented in Fig. 5. Synchronization of the pulses with the *d*-axis is ensured by measuring of θ_1 (for VSC1) and θ_2 (for VSC2) with PLL blocks. Noting that 16 pulse generation circuits similar to this one are required for BtB-STATCOM operation.

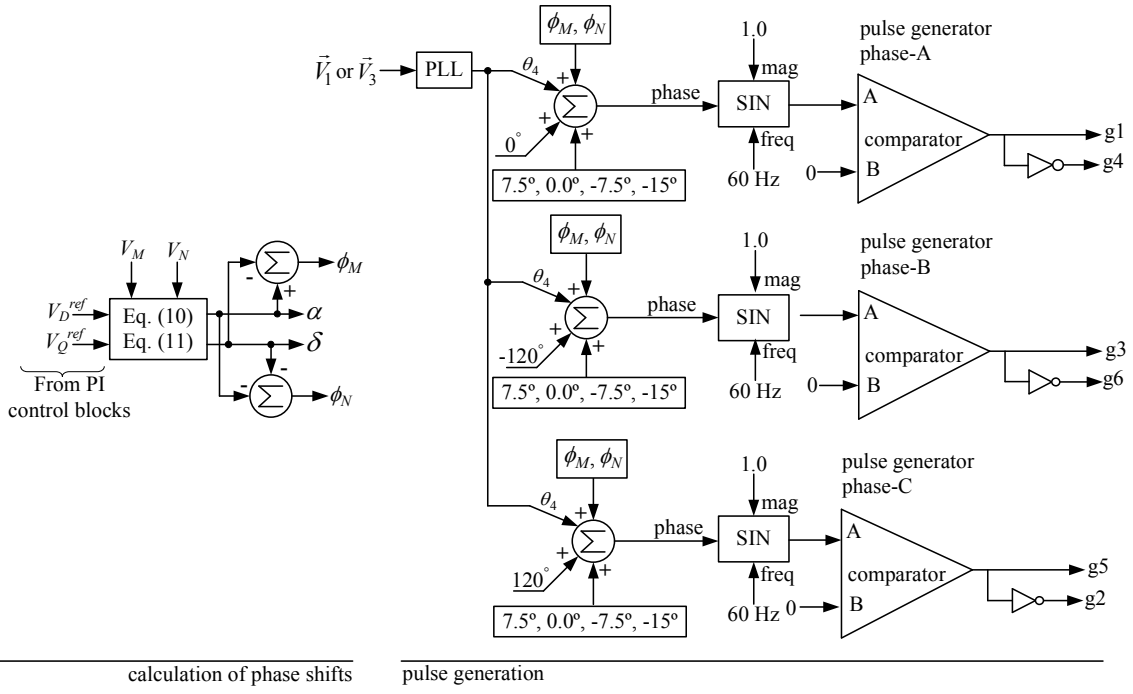

Fig. 5 Pulse generator circuit for two-level six-pulse converter

V. Simulation Results and Discussion

The validity of the proposed BtB-STATCOM and its control schemes are tested through comprehensive simulation cases in a multi-machine power system (base power: 100 MVA at 60 Hz, transmission level: 154 kV) with a solution time step of 20 us in PSCAD/EMTDC. This power network resembles a small portion of the central New York State transmission system in much simplified way [22]. The system

is mainly constructed by standard blocks of PSCAD main library. Transmission lines are modelled by standard coupled pi section and loads are modelled as constant PQ absorbing modules. Parameters of the system are given in Appendix. DC link voltage is controlled at 2.0 kV throughout all simulation cases.

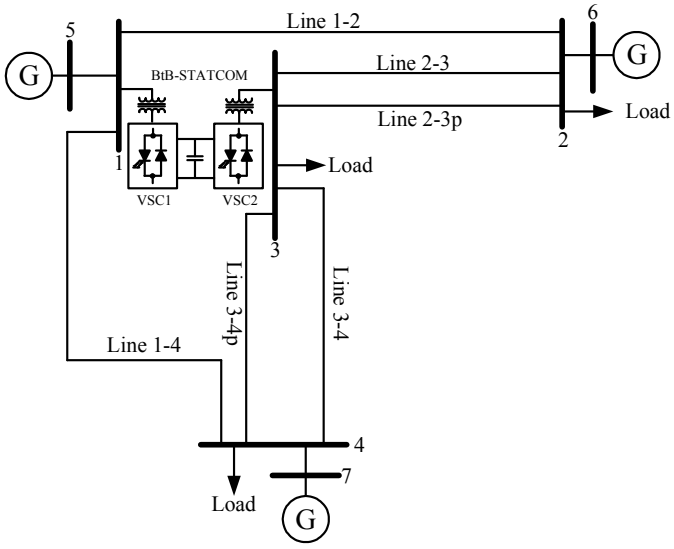

Fig. 6 BtB-STATCOM with multi-machine power system

A. Case1: Start-up transients

BtB-STATCOM is started up to control bus voltages (V_1 and V_3) at 1.0 pu and to enable real power transfer between Bus 1 & 3. Noting that uncontrolled bus voltages are 0.99 pu and 0.97 pu, respectively. Real power transfer ($P_{transfer2}$) is set at 0.5 pu. Since start-up transients are highly dependent upon voltage ramp up time of the generators in PSCAD/EMTDC, a ramp-up time of 0.05 s, divisible into the period of the fundamental frequency, is selected [23]. The results are graphically presented in Fig. 7(a)-(j). No overshoot is observed in the tracking signals of bus voltages in Fig. 7(a)-(b). V_1 and V_3 come to their desired values with no steady-state error within 0.06 s and 0.8 s, respectively. This is due to different reactive power requirements of each bus. The steady-state magnitudes of injected reactive powers into Bus1 and Bus3 are 13 MVar and 65 MVar, respectively. Fig. 7(c) shows the response of the real power transfer from Bus1 to Bus3 to a step change of 0.5 pu (50 MW) at $t=0^+$. After 1.4 s, real power flow comes to its desired value with no overshoot. The DC link voltage regulation is a key factor for the successful operation of voltage source based converters. On account of this, E is tightly regulated at 2.0 kV (Fig. 7(d)). Actual DC link voltage settles on 2.0 kV line within 0.2 s. Figs. 7(e)-(j) show some related signals taken from the simulation.

B. Case 2: Response of step changes to the real power transfer reference

BtB-STATCOM is commanded to reverse real power transfer between Bus 1 and Bus 3 from 0.4 pu to -0.4 pu at 4.0 s and restore it back to its previous value at 6.0 s. The other reference points of BtB-STATCOM control loops are kept unchanged as in case 1. Fig. 8(a)-(h) show the traces of this case study. Fig. 8(a) shows that real power transfer reaches to its commanded values in around 1.0 s after the step change command has been applied. The response is robust with no steady-state error. The DC link voltage stays constant after following a 20 % undershoot and 25 % overshoot. The response of V_1 and V_3 is constant on 1.0 pu line and not shown here. Although practical PI controllers are utilized, all responses regarding this case study exhibit stable performance. BtB-STATCOM is able to reverse the direction of real power transfer between neighbouring buses without disturbing other control parameters.

C. Case 3: Single-phase to earth fault

The dynamic performance of the BtB-STATCOM is evaluated by applying phase-A to earth fault at the middle of the Line 2-3 at 10.5 s for 100 ms and cleared without any change in the network configuration. Probability of realization of such a disturbance is high as the ratio of single-phase to earth faults is about 80-81 % of fault types [24]-[25]. The reference values of all control loops of BtB-STATCOM are kept constant as in case 1. Fig. 9(a)-(j) show simulated responses to the fault. The rms voltage magnitudes of compensated buses without/with BtB-STATCOM are compared and presented in Fig. 9(a)-(b). V_1 and V_3 returns to their controlled values within 1.0 s after the fault is cleared and an overshoot of less than 0.25 % and 2.5% is observed, respectively. Voltage sag does not go below more than 0.5 % of nominal value of V_1 and 7.5 % of nominal value of V_3, respectively. For both measurements, BtB-STATCOM could hold voltage levels higher than the uncompensated case during fault. Real power transfer drops around 17.0 % of its nominal value during fault but it restores within 1.65 s with an overshoot of 2.5 % after the fault is cleared. PI control could hardly keep DC link voltage at its steady-state value against sustained oscillation, but DC link voltage returns to its controlled value within around 0.7 s following after the fault. It has been deduced that the magnitude of the real power transfer is inversely proportional to the DC link voltage controller performance. Tracking performances of all PI controllers show that the controlled parameters do not pass to unstable region even though the controllers have simple structure in nature. Fig. 9(e)-(j) demonstrates some recorded signals of BtB-STATCOM related with this case study.

D. Case 4: Three-phase short circuit

A three-phase short circuit (the most severe disturbance) with the occurrence probability of 1.5-3.0% [24]-[25] is applied to the middle of the Line 2-3 at 10.5 s for 100 ms and cleared. The reference values of all control loops of BtB-STATCOM are kept constant as in case 1. Fig. 10(a)-(j) show comparative simulated responses to the short circuit. Voltage sag less than 1.5 % and swell no more than 1.0 % have been recorded for V_1 in Fig. 10(a). BtB-STATCOM retrieves the voltage magnitude to its controlled value in less than 1.5 s. In Fig. 10(b), voltage sag for Bus 3 goes 40% of nominal value and recovers in around 1.5 s after the fault is cleared. Real

power transfer is severely disturbed since Bus 3 is next to the fault location. It drops to a negative value that the direction of flow has been temporary reversed from 40 MW to -4 MW due to fault. The disturbance lasts no more than 2.5 s. Combining Fig. 9(c) and Fig. 10(c), the excursions occurred in real power transfer for this case study is more than those of case 3. DC link voltage recorded in Fig. 10(d) is more ludic than the trace observed during phase-A to earth fault condition (Fig. 9(d)). The performances of PI controllers are relatively poor in case of three-phase fault but without losing stability. Fig. 10(e)-(j) also present some recorded signals of BtB-STATCOM related with this case study.

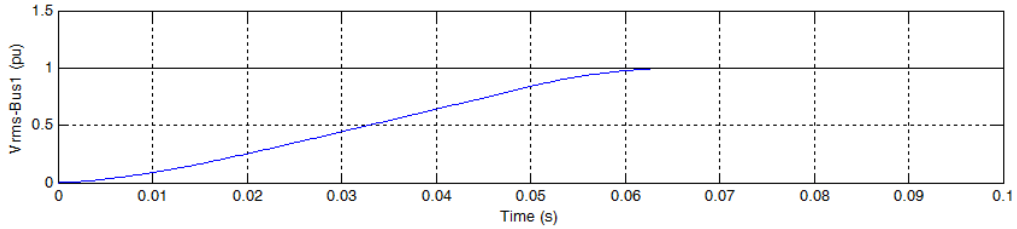

(a) Bus 1 line-to-line rms voltage control by BtB-STATCOM at start-up for a step-change of 1.0 pu

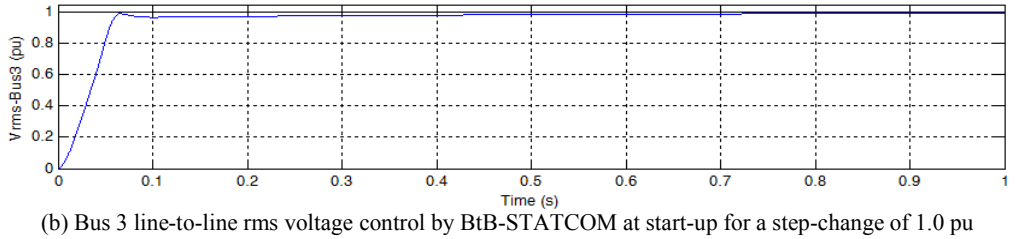

(b) Bus 3 line-to-line rms voltage control by BtB-STATCOM at start-up for a step-change of 1.0 pu

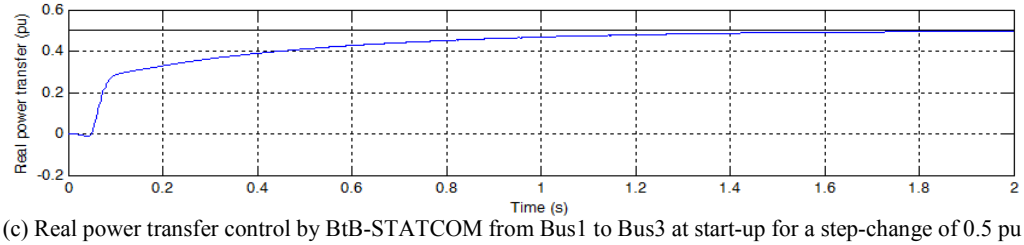

(c) Real power transfer control by BtB-STATCOM from Bus1 to Bus3 at start-up for a step-change of 0.5 pu

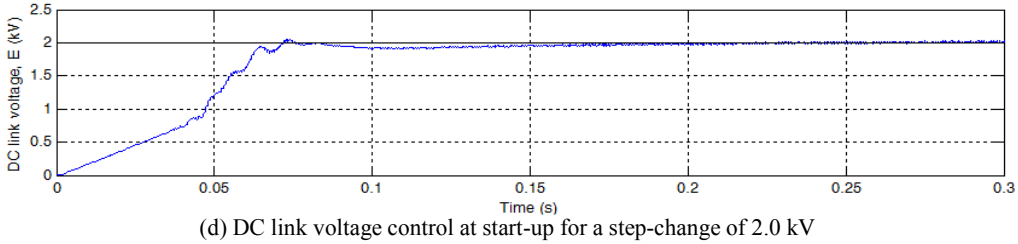

(d) DC link voltage control at start-up for a step-change of 2.0 kV

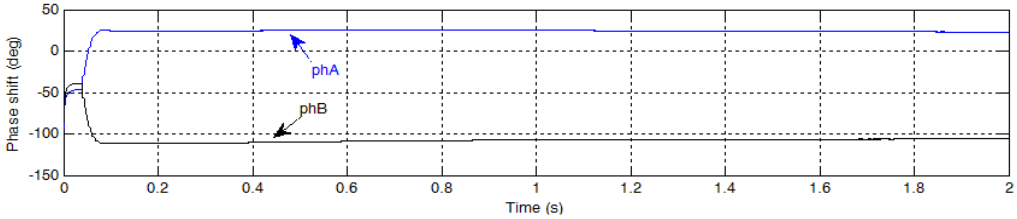

(e) Calculated phase shifts for converter M & N of VSC1 (phA=Φ_M and phB=Φ_N) during start-up

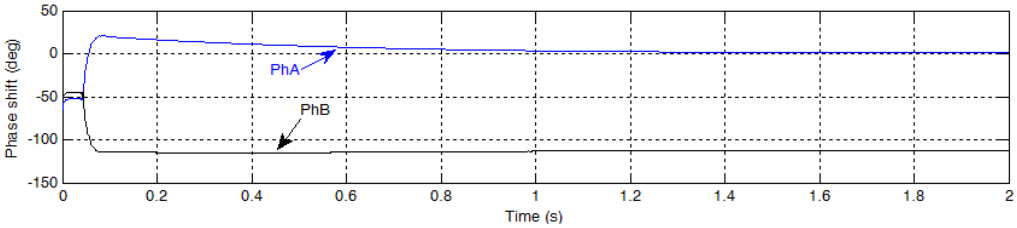

(f) Calculated phase shifts for converter M & N of VSC2 (phA=Φ_M and phB=Φ_N) during start-up

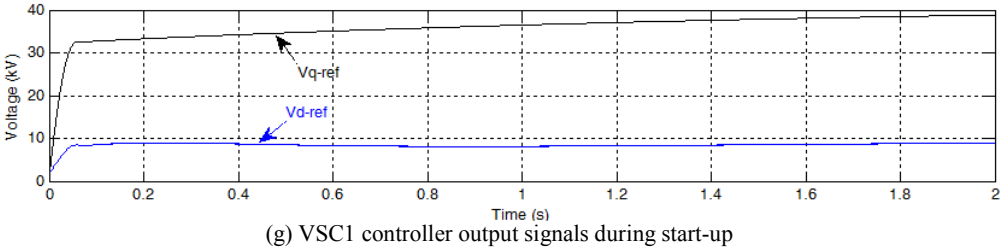

(g) VSC1 controller output signals during start-up

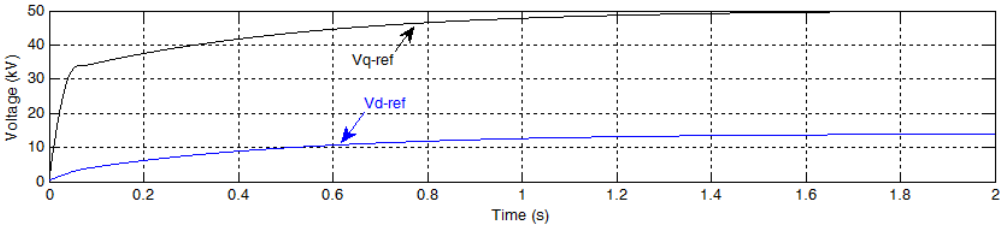

(h) VSC2 controller output signals during start-up

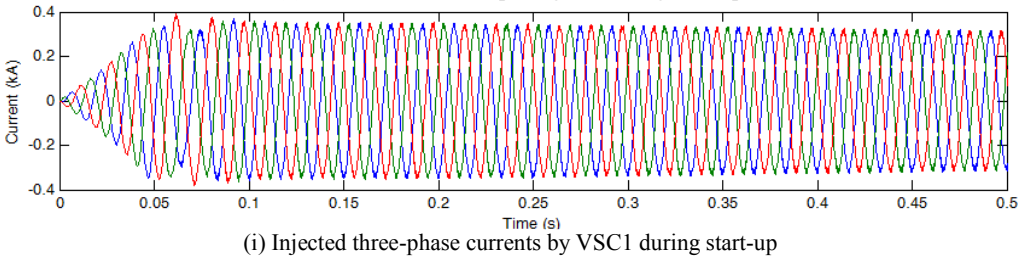

(i) Injected three-phase currents by VSC1 during start-up

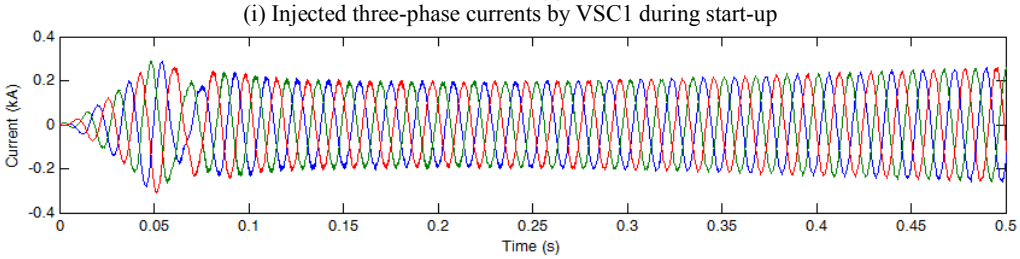

(j) Injected three-phase currents by VSC2 during start-up

Fig. 7 Simulated waveforms of start-up transients (Case 1)

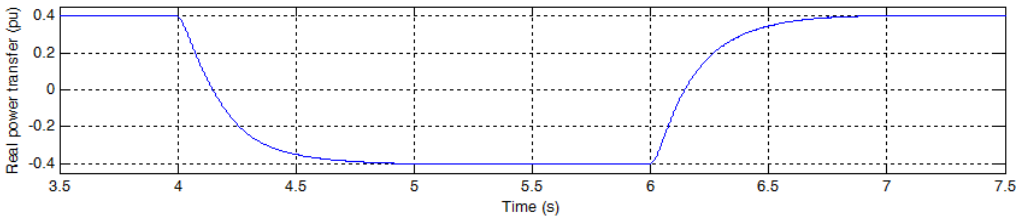

(a) Reversing real power transfer by BtB-STATCOM from Bus1 to Bus3

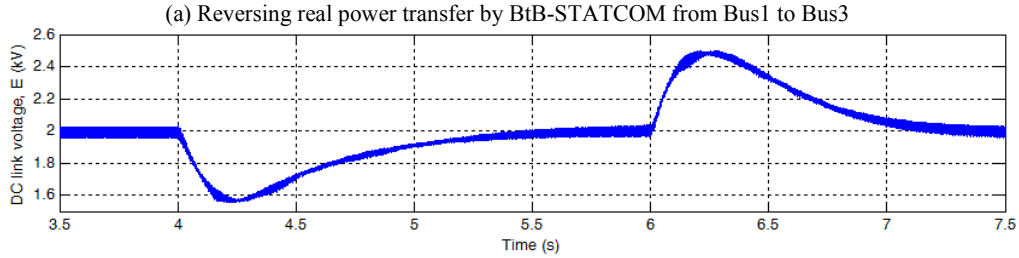

(b) DC link voltage transients

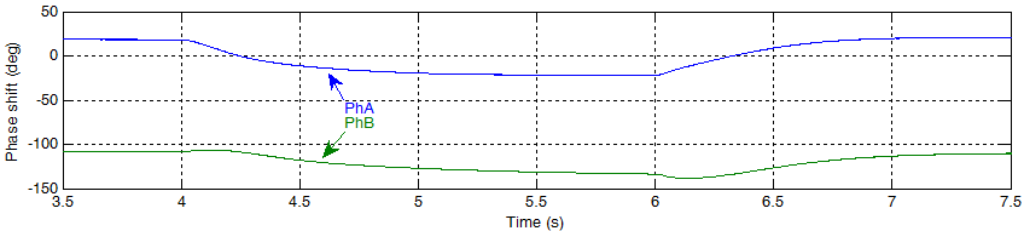

(c) Calculated phase shifts for converter M & N of VSC1 (phA=Φ_M and phB=Φ_N)

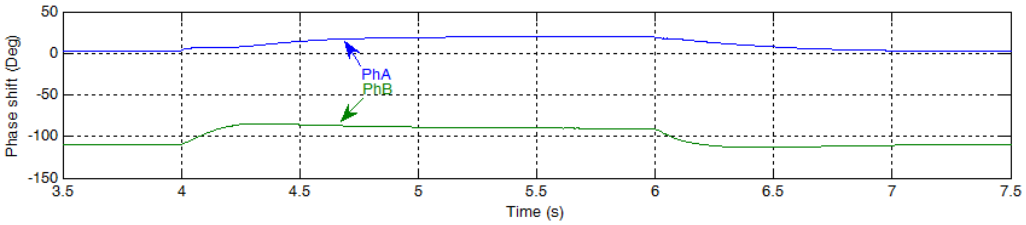

(d) Calculated phase shifts for converter M & N of VSC2 (phA=Φ_M and phB=Φ_N)

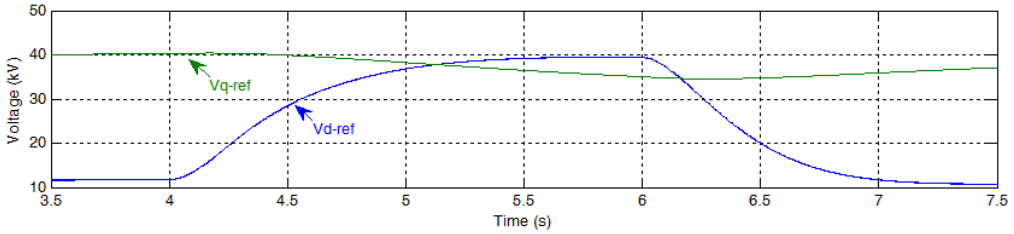

(e) VSC1 controller output signals

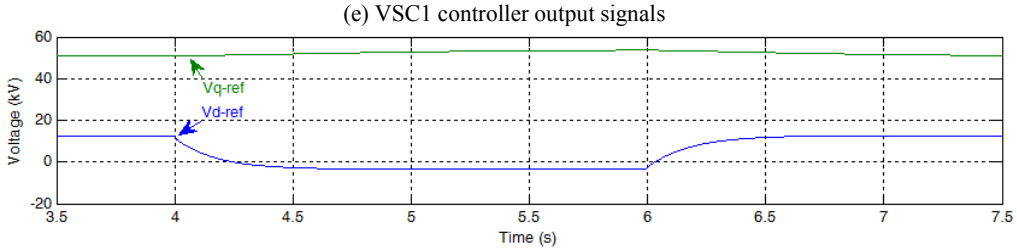

(f) VSC2 controller output signals

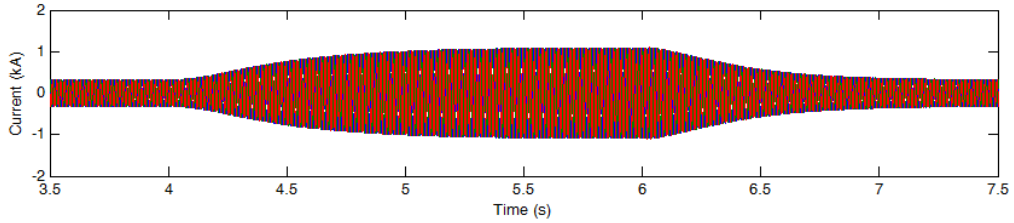

(g) Injected three-phase currents by VSC1 reversing real power transfer

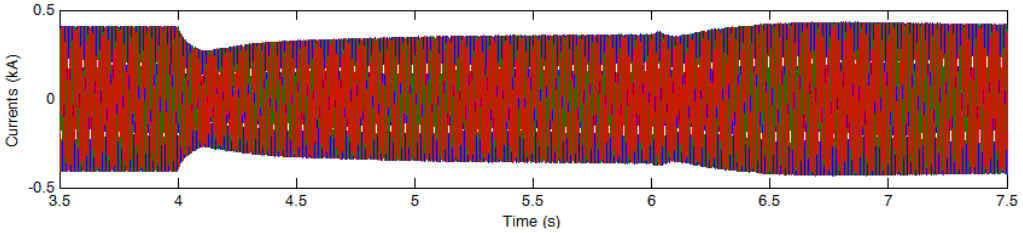

(h) Injected three-phase currents by VSC2 reversing real power transfer.

Fig. 8 Simulated waveforms during reversal of real power transfer (Case 2)

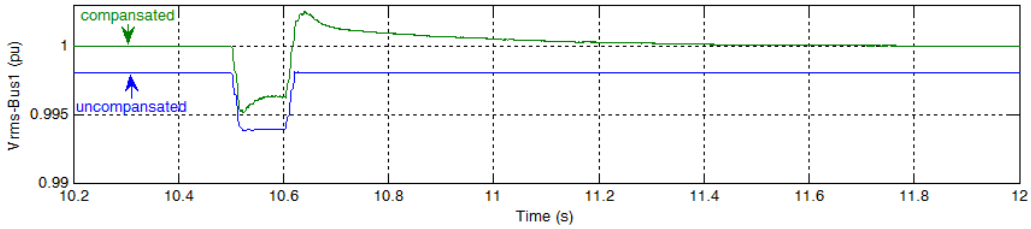

(a) Bus 1 voltage response to phase-A to earth fault at 10.5 s

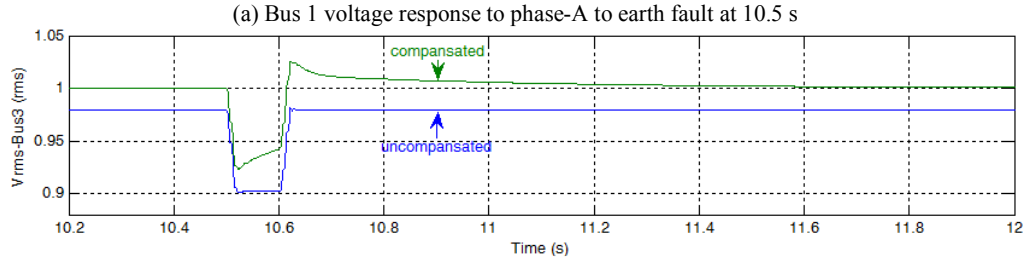

(b) Bus 3 voltage response to phase-A to earth fault at 10.5 s

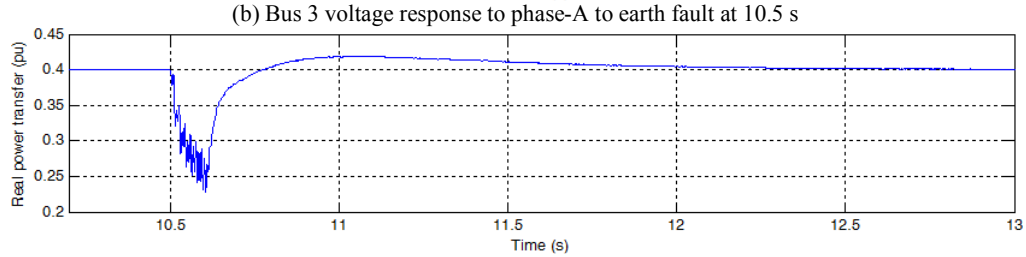

(c) Real power transfer response to phase-A to earth fault at 10.5 s

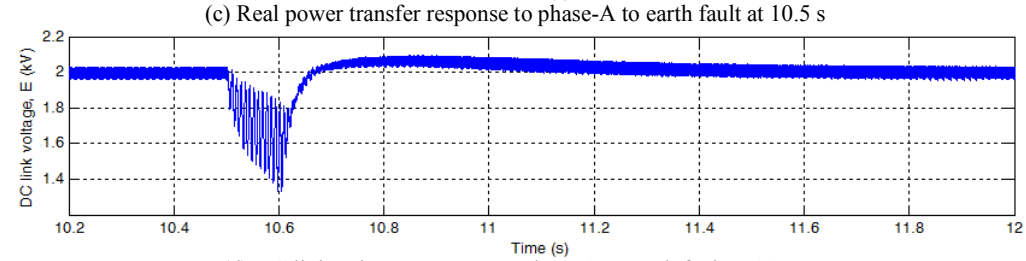

(d) DC link voltage response to phase-A to earth fault at 10.5 s

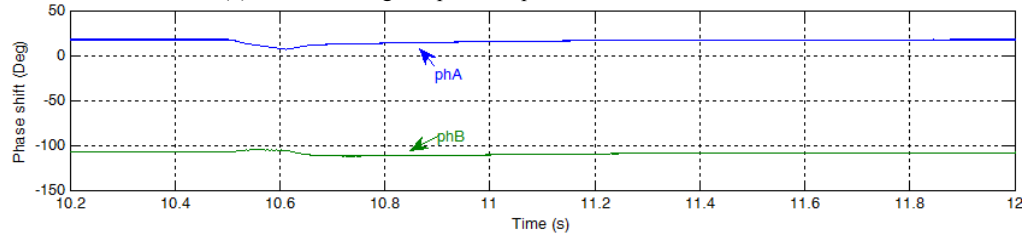

(e) Phase-shift angles of VSC1 in response to phase-A to earth fault at 10.5 s. (phA=Φ_M and phB=Φ_N)

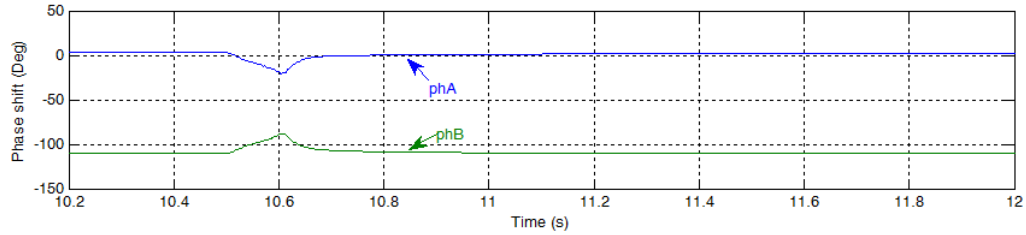

(f) Phase-shift angles of VSC2 in response to phase-A to earth fault at 10.5 s. (phA=Φ_M and phB=Φ_N)

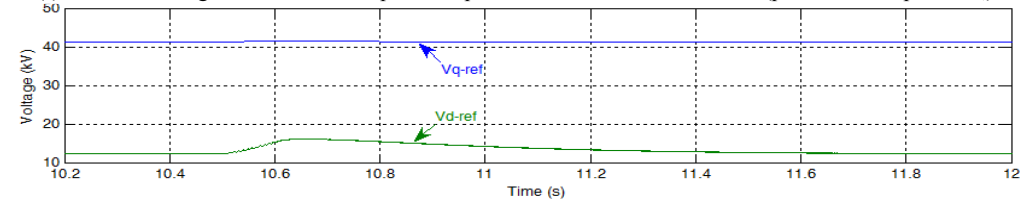

(g) VSC1 controller output signals in response to phase-A to earth fault at 10.5 s

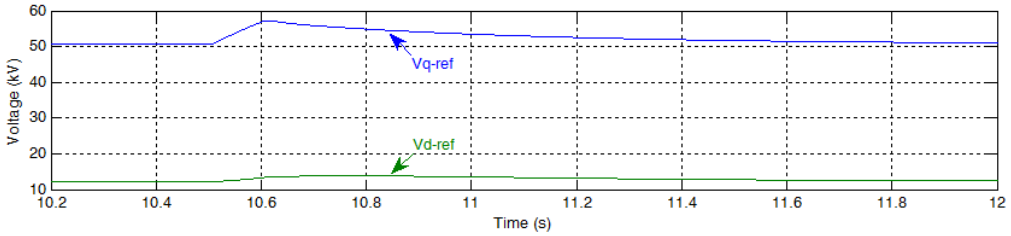

(h) VSC2 controller output signals in response to phase-A to earth fault at 10.5 s

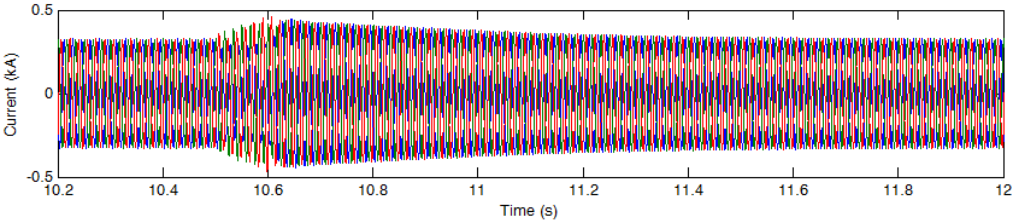

(i) Three-phase injected currents into Bus1 in response to phase-A to earth fault at 10.5 s

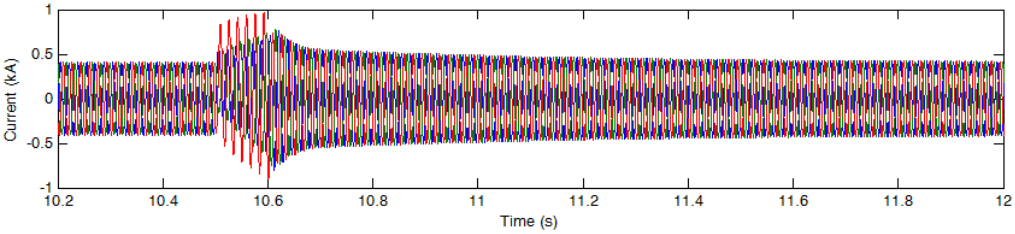

(j) Three-phase injected currents into Bus3 in response to phase-A to earth fault at 10.5 s

Fig. 9 Simulated waveforms during phase-A to earth fault (Case 3)

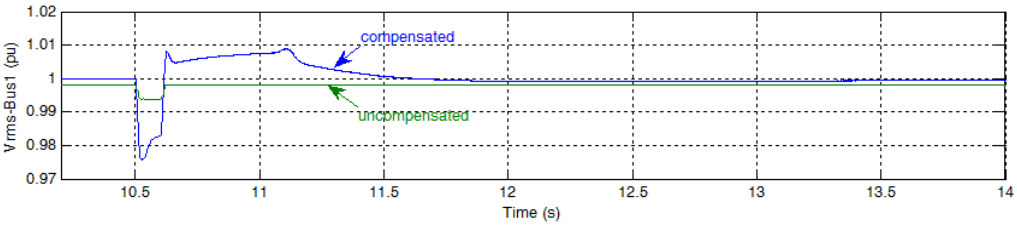

(a) Bus 1 voltage response to three-phase fault at 10.5 s

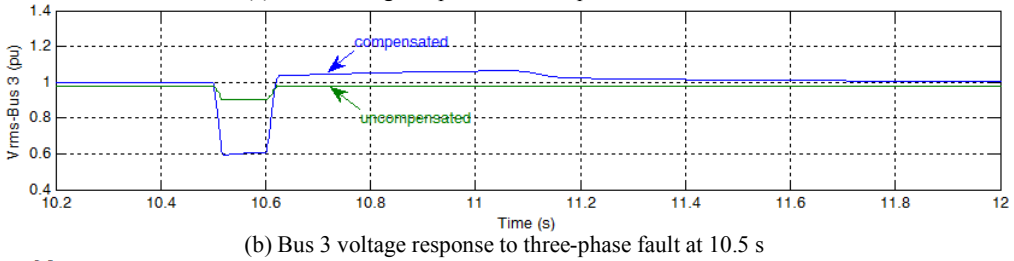

(b) Bus 3 voltage response to three-phase fault at 10.5 s

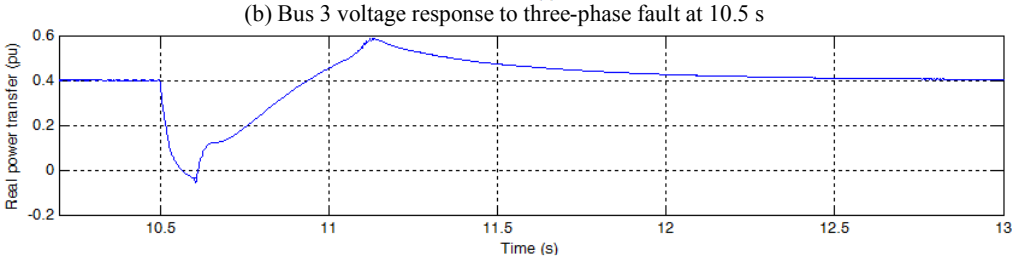

(c) Real power transfer response to three-phase fault at 10.5 s

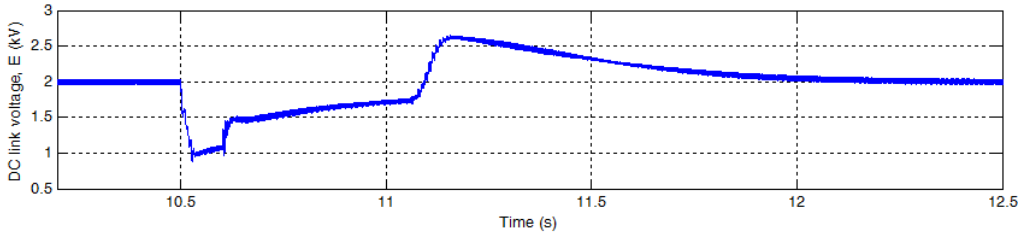

(d) DC link voltage response to three-phase fault at 10.5 s

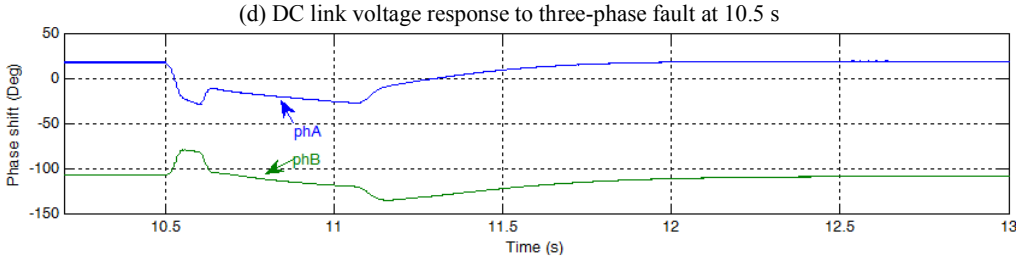

(e) Phase-shift angles of VSC1 in response to three-phase fault at 10.5 s. (phA=Φ_M and phB=Φ_N)

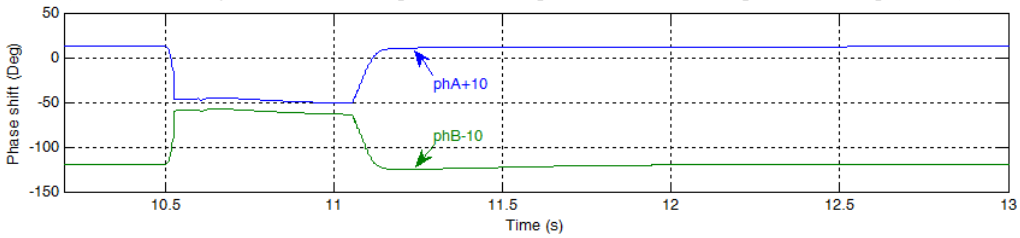

(f) Phase-shift angles of VSC2 in response to three-phase fault at 10.5 s. (phA=Φ_M and phB=Φ_N)

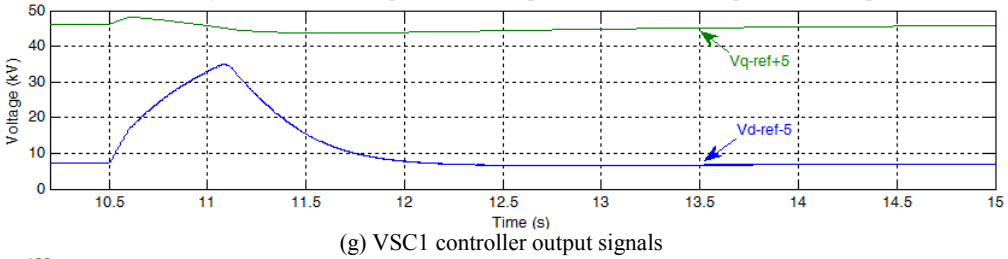

(g) VSC1 controller output signals

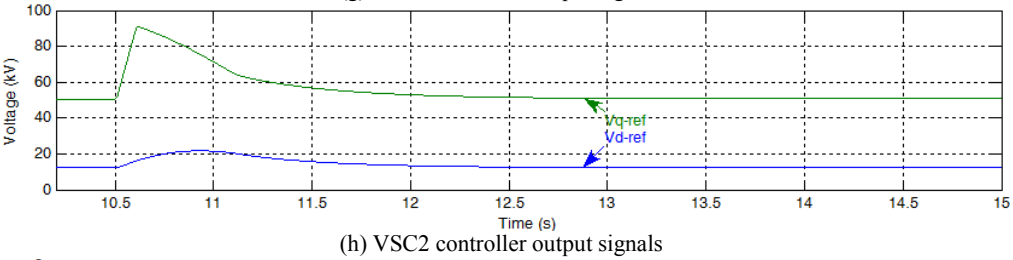

(h) VSC2 controller output signals

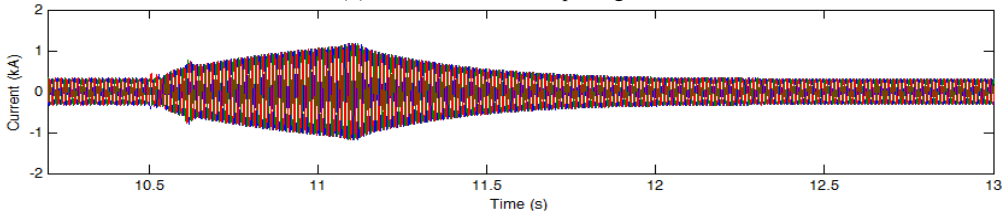

(i) Three-phase injected current into Bus1 in response to three-phase fault at 10.5 s

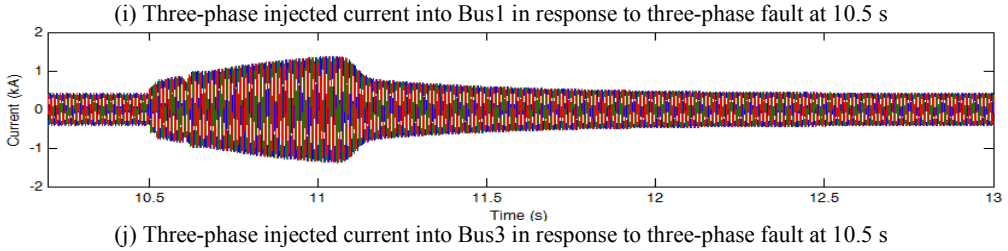

(j) Three-phase injected current into Bus3 in response to three-phase fault at 10.5 s

Fig. 10 Simulated waveforms during three-phase fault (Case 4)

E. Case 5: THD Content

Table I shows THD of voltages/currents during BtB-STATCOM steady-state operation in case 1. The voltage/current harmonics are within acceptable limits of IEEE-519 standard [26].

TABLE I
THD CAUSED BY BTB-STATCOM

%THD	Bus1	Bus3
Bus Voltage	0.33	0.30
Injected Current	1.60	1.22

VI. CONCLUSION

Quasi multi-pulse VSC, pulse generating circuits, and control schemes for BtB-STATCOM has been designed and verified through different simulation scenarios in PSCAD/EMTDC. Independent control of voltage magnitude and phase angle of the converters without high frequency pulse width modulation makes the use of separate control for active and reactive power possible. Conventional PI controllers are robust and yet practically applicable to voltage magnitude and real power transfer control owing to their simplicity. THD levels of the two converters comply with the regulations even the switching is made at low frequency. This study can easily be extended to VSC-HVDC transmission with DC transmission lines. Moreover, with back-to-back converters it is also possible to supply a fixed amount of bi-directional power flow between micro-macro grid.

APPENDIX

MULTI-MACHINE SYSTEM DATA (SBASE=100 MVA)

Line Name	R (Ω)	Line Name	R (Ω)
1-2	1.78	31.4	1.83E-4
1-4	1.13	19.9	1.16E-4
1-5	-	0.237	-
2-3	1.25	22.0	1.28E-4
2-3p	1.25	22.0	1.28E-4
2-6	-	0.047	-
3-4	1.25	22.0	1.28E-4
3-4p	1.25	22.0	1.28E-4
4-7	-	0.047	-
Load Location	Load		
@ Bus 2	0.15+j0.5 pu		
@ Bus 3	1.25+j0.5 pu		
@ Bus 4	0.9 + j0.3 pu		

REFERENCES

[1] X. Fang, J.H. Chow, "BTB DC link modeling, control, and application in the segmentation of AC interconnections," *IEEE Power & Energy Society General Meeting*, pp.1-7, July 2009.

[2] S. Ruihua, Z. Chao, L. Ruomei, Z. Xiaoxin, "VSCs based HVDC and its control strategy," *IEEE Transmission and Distribution Conference and Exhibition*, pp.1-6, 2005.

[3] M.R. Banaei, N. Taheri, "HVDC based damping controllers for power system stability," 31st International Telecommunications Energy Conference, pp.1-6, October 2009.

[4] B. Parkhideh, S. Bhattacharya, "Resilient operation of voltage-sourced BTB HVDC systems under power system disturbances," *IEEE Power & Energy Society General Meeting*, pp.1-7, July 2009.

[5] K.K. Sen, M.L. Sen, Introduction to FACTS Controllers: Theory, Modeling, and Applications, Wiley Blackwell, 2009.

[6] A. Gelen, T. YALÇINÖZ, "Experimental studies of a scaled-down TSR-based SVC and TCR-based SVC prototype for voltage regulation and compensation", *Turkish Journal of Electrical Engineering & Computer Sciences*, Vol. 18, No.2, pp. 147-158, 2010.

[7] P. R. Sharma, A. Kumar, N. Kumar, "Optimal Location for Shunt Connected FACTS Devices in a Series Compensated Long Transmission Line, *Turkish Journal of Electrical Engineering & Computer Sciences*, Vol. 15, No.3, pp. 321-328, 2007

[8] N. Flourentzou, V.G. Agelidis, G.D. Demetriades, "VSC-Based HVDC Power Transmission Systems: An Overview", *IEEE Trans. on Power Electronics*, Vol.24, No.3, pp.592-602, 2009.

[9] A. Tyagi, K.R. Padiyar, "Dynamic analysis and simulation of a VSC based Back-to-Back HVDC link", *India International Conference on Power Electronics,* pp.232-238, 2006.

[10] N. Ottosson, L. Kjellin, "Modular back-to-back HVDC, with capacitor commutated converters (CCC)," *Seventh International Conference on AC-DC Power Transmission,* pp. 55-59, November 2001.

[11] G. Reed, R. Pape, M. Takeda, "Advantages of voltage sourced converter (VSC) based design concepts for FACTS and HVDC-link applications," *IEEE Power Engineering Society General Meeting,* Vol. 3, No. 4, pp. 1821, July 2003.

[12] D. Kidd, B. Mehraban, B. Ekehov, J. Ulleryd, A. Edris, "Eagle pass back to back VSC installation and operation," *IEEE Power Engineering Society General Meeting,* Vol. 3, pp. 1829-1833, July 2003.

[13] M. Hagiwara, V.P. Phuong. H. Akagi, "Calculation of DC Magnetic Flux Deviation in the Converter-Transformer of a Self-Commutated BTB System During Single-Line-to-Ground Faults," *IEEE Trans. on Power Electronics,* Vol. 23, No. 2, pp.698-706, March 2008.

[14] "The FACTS on resolving transmission gridlock," *IEEE Power and Energy Magazine,* Vol. 1, No. 5, pp. 41-46, 2003.

[15] R. Majumder, M. Dewadasa, A. Ghosh, G. Ledwich, F. Zare, "Control and protection of a microgrid connected to utility through back-to-back converters", *Electric Power Systems Research*, Vol. 81, Issue 7, pp. 1424-1435, July 2011.

[16] A. Chakraborty, "Advancements in power electronics and drives in interface with growing renewable energy resources", *Renewable and Sustainable Energy Reviews*, Vol. 15, Issue 4, pp. 1816-1827, May 2011.

[17] O. Gomis-Bellmunt, A. Junyent-Ferre, A. Sumper, J. Bergas-Jane, "Control of a Wind Farm Based on Synchronous Generators With a Central HVDC-VSC Converter", *IEEE Trans. on Power Systems*, Vol. 26, No. 3, pp.1632-1640, August 2011.

[18] M. Hagiwara, H. Fujita, H. Akagi, "Performance of a self-commutated BTB HVDC link system under a single-line-to-ground fault condition", *IEEE Trans. on Power Electronics,* Vol. 18, No. 1, pp. 278-285, January 2003.

[19] D. Soto, T.C. Green, "A comparison of high-power converter topologies for the implementation of FACTS controllers", *IEEE Trans. on Industrial Electronics*, Vol. 49, No. 5, pp. 1072-1080, October 2002.

[20] C.K. Lee, J.S.K. Leung, S.Y.R. Hui, H.S.-H Chung, "Circuit-level comparison of STATCOM technologies", *IEEE Trans. on Power Electronics* , Vol. 18, No. 4, pp. 1084- 1092, July 2003.

[21] L. Zhang, H.-P. Nee, "Multivariable feedback design of VSC-HVDC connected weak AC systems", *IEEE PowerTech*, pp. 1-8, 2009.

[22] B. Fardanesh, "Optimal utilization, sizing, and steady-state performance comparison of multiconverter VSC-based FACTS controllers", *IEEE Trans. on Power Delivery*, Vol. 19, No. 3, pp. 1321-1327, July 2004.

[23] PSCAD/EMTDC: Electromagnetic Transients Program Including DC Systems Manitoba HVDC Research Centre, 1994.

[24] P. Heine, M. Lehtonen, "Voltage sag distributions caused by power system faults", *IEEE Trans. on Power Systems*, Vol. 18, No. 4, pp. 1367-1373, November 2003.

[25] U.A. Bordalo, A.B. Rodrigues, M.G. Silva, "A new methodology for probabilistic short-circuit evaluation with applications in power quality analysis", *IEEE Trans. on Power Systems,* Vol. 21, No. 2, pp. 474- 479, May 2006

[26] IEEE Standard 519-1992, *IEEE Recommended Practices and Requirements for Harmonic Control in Electrical Power Systems*, IEEE Inc., New York, 1992.